



The expression characteristics and allelic variation of *AnVromindoline-1/3* in *Avena nuda* L.

Jiang-hong An · Jin-sheng Nan · Hui-yan Liu ·
Ming-na Chai · Bing Han · Yan Yang

Received: 24 October 2022 / Accepted: 11 October 2023 / Published online: 20 November 2023
© The Author(s) 2023

Abstract Oat is a worldwide cultivated crop with nutritional, ecological and economic value. The hardness of oat is closely related to the damage to the grain during harvesting, washing, threshing and hulling, and has an important impact on the processing quality and eating quality of oats. Vromindolines are a group of proteins specific to the *Avena* genus and are responsible for the softness of oat endosperm. *Avena nuda* is an allohexaploid, and is an important grain and feed crop in China. Vromindolines have been studied in the genus Oat, but have not been reported in *Avena nuda*. In this study, we performed paraffin sectioning and scanning electron microscopy analysis on oat kernels with different hardness, and the sequence characteristics, allelic variation, expression

patterns and subcellular localization of *Vromindoline-1* and *Vromindoline-3* genes in *Avena nuda* were also analyzed. The results showed that the cell structure and ultrastructure of soft oat variety grains are significantly different from those of hard oats variety. PCR amplification and sequence analysis showed that the lengths of *AnVin-1* and *AnVin-3* genes were 444 and 429 bp, respectively, and *AnVin-1* existed in the oat A, C and D genomes. Expression analysis in different tissues showed that *AnVin-1A*, *AnVin-1C*, *AnVin-1D* and *AnVin-3C* were expressed to varying degree in roots, stems and leaves. Expression analysis at the panicle developmental stage showed that the expression levels of these four genes first increased and then decreased, with the highest expression levels at 14 days after pollination. In addition, the expression levels of *AnVin-1C* and *AnVin-3C* in soft oat variety were higher than those in hard oats at 14 DAP. Among the single nucleotide polymorphisms among 18 *AnVin-1C* and 9 *AnVin-3C* gene sequences, *AnVin-1C6* and *AnVin-3C2* genes had three haplotypes in a oat natural population. Based on the allelic variation sites of *AnVin-1C6*, a cleavage amplified polymorphic sequence marker was established, which explained 1.44% of the variation in hardness. The above results of this study indicated that *AnVin-1* and *AnVin-3* genes were involved in kernel development and might affect kernel firmness.

Supplementary Information The online version contains supplementary material available at <https://doi.org/10.1007/s10681-023-03251-9>.

J. An · J. Nan · H. Liu · M. Chai · B. Han (✉) ·
Y. Yang (✉)

Key Lab of Germplasm Innovation and Utilization of Triticeae Crop at Universities of Inner Mongolia Autonomous Region, Inner Mongolia Agricultural University, Hohhot 010018, China
e-mail: hb_nmg@163.com

Y. Yang
e-mail: yangyanchutao@126.com

J. An
Inner Mongolia Academy of Agricultural and Animal Husbandry Sciences, Hohhot 010031, China

Keywords *Avena nuda* L. · Kernel hardness · *Vromindoline* · Alleles · Gene expression

Introduction

Among the cereal crops, oat is characterized by a soft endosperm texture, which has a negative impact on the industrial processing of oats, such as reduced oatflake yield (Alfieri et al. 2014). The single kernel characterization system (SKCS) is usually used to determine the hardness value of oat (Gazza et al. 2015) and has certain advantages in measuring hardness (Jianghong et al. 2020). Our previous research compared the accuracy of SKCS and Texture Analyzer (TA), the results showed that TA method was more suitable in detecting the kernel hardness of *A. nuda* (Jianghong et al. 2021).

The endosperm texture is the result of the combined effect of the biomolecular composition of the grain (Chunqing 1992). Wheat kernel hardness depends on the cohesion between the starch granules, the protein matrix, and the continuity of the protein matrix that coats the starch granules (Greenwell & Schofield 1986). Both genotype and environment affect kernel hardness values, with genotype having a greater effect (Shihua 2003; Shihua et al. 2005). For example, puroindoline genes that were mapped to the *Ha* locus on the wheat chromosome 5D (Giroux & Morris 1998) explain 63.2% of the total variation in hardness (Sourdille et al. 1996).

Vromindolines are proteins coded for by the *Vromindoline* (*Vin*) gene family, which had been investigated in *Avena* species at different ploidy levels (except for *Avena nuda*) and shown to be responsible for the soft endosperm texture of oats (Gazza et al. 2015). In *A. sativa*, three *Vin-1* genes, three *Vin-2* genes, and two *Vin-3* genes have been characterized and assigned to A, C, or D genomes based on similarity to their counterparts in diploid species (Gazza et al. 2015). The sequences of various vromindoline proteins of different species differ mainly due to amino acid changes caused by single base pair variations (Alfieri et al. 2014; Gazza et al. 2015).

In this study, *A. nuda* oats were planted in two ecological areas for three consecutive years (2019–2021) to obtain an adequate amount of mature seeds for hardness measurements. Materials with significantly different hardness values were selected for gene cloning, expression pattern analysis, allelic variation analysis and development of molecular markers related to grain hardness. This study characterized *Vin-1* and *Vin-3* genes in *A. nuda*, providing information for

future research on the control of the grain texture of oat.

Materials and methods

Plant material

A total of 260 *A. nuda*, containing cultivars, landraces, and varieties imported from abroad, were planted in Bashang of Hebei Province (114°42'54" E, 41°4'6" N) and Ulanqab of Inner Mongolia (113°13'59" E, 40°56'50" N) in 2019, 2020, and 2021 (Supplementary file 1). The elementary plot of 1 m² consisted of three rows, 30 cm apart, sown with 350 germinating kernels/m².

Kernel hardness determination of oat

The grain harvested at two locations in 2019, 2020, and 2021 were tested for kernel hardness values. Broken, coarse, and small kernels were discarded, and one hundred grains were randomly selected for repeated tests of kernel hardness, which were evaluated by TA (TA-XT PLUS) (Jianghong 2022).

Preparation of paraffin sections and scanning electron microscopy (SEM) of mature grains

Mature grains were immersed in 4% paraformaldehyde fixative solution and breezed overnight at 4 °C. The samples were sent to Beijing GenePool Biotechnology Co., Ltd. for paraffin sectioning and staining with hematoxylin. Mature, dry grains of naked oats were directly cut with a sharp blade. Sections of 1 mm were cut from each sample, and the bottom of the sample was fixed on the sample table with conductive adhesive. The samples were viewed using a TM4000pLUS scanning electron microscope (SEM) operating at 10 kV. The magnification level is 600x.

DNA extraction and PCR amplification

Genomic DNA was isolated from young leaves of all tested materials using the cetyltrimethylammonium bromide (CTAB) method (Turaki et al. 2018). The sequences of gene-specific primers are listed in Table 1. PCR reactions were performed in a Veriti™ 96-Well Thermal Cycler in a total volume of 25 µL.

Table 1 The primer sequences used in this study

Primer name	Upstream primer (5'–3')	Downstream primer(5'–3')	Tm/°C	Product size/bp
Vin-1F/R	GAAACATGAAGACCTTACTGC	CCAGTAGTAGCCAGTAGTAAG	58	441
Vin-3F/R	ATGAAGGCCTTATTCCTCCTAGCTT	GTAATATCCAAGATTGGTAGGGAAG	58	429
Vin-1A1F/R	GAGACAAAGAACCATGGCTG	ATCCACTTCCACTCCCTTTTTTC	59	1082
Vin-1C1F/R	TCACCTAGTCTATAAATCGTGTC	CTTTCATCCTCTTCGTTCTC	56	754
Vin-1D1F/R	AGCCAAAGGAACACATAATGG	CGGCTAGCTAGATTTCACGC	58	872
Vin-1A2F/R	ATGAAGACCTTACTGCTCTTAGCTC	GGTGAAGCATCGCTGCG	62	172
Vin-1C2F/R	TGCTCTTAGCTGTGCTAGCTCTC	ACTGCTGCGACACCTGGTTC	62	264
AsActin	CCTCACAACAACCGCTGAGC	CTCATACGATCAGCAATTCAGGAA	60	348
Vin1C-133F/R	GCTATTCATATTCACCTTCACGGG	ATCGAGTGGTAGAAAGTAGCACC	64	536
Vin1C-3F/R	CGAGCACCGCCTTCGCG	AGGAACCCGCCGAGCTCGT	66	290
Vin1C-94F/R	AGCGGCAGGATGCGCGT	ACTGGGGCCCCATGTCT	64	312
Vin1C-101F/R	TCACCTAGTCTATAAATCGTGTC	TCTTGTTCCTTAAGACTCAAAGAACC	66	732
Vin1D-9F/R	AGCCAAAGGAACACATAATGG	TTGGATTTAATTGTTATGTGAATGT	62	835
Vin1D-17F/R	CACTAGCATCATGAAGACCTTCCG	ACGTAATCCTTGCAAGAGTGGT	62	162
Vin1D-56F/R	GCGGAGAAGCGATAGGATCT	CACACACACAACCACCAAGAATG	65	501
Vin1D-29F/R	AGCCAAAGGAACACATAATGG	TATTAACAGAGCATAAAGACTCGGG	64	727
Vin3C-16F/R	ATGAAGGCCTTATTCCTCCTAGCTT	GCAGCACTGGGCTCGTG	66	383
Vin3C-26F/R	ATGAAGGCCTTATTCCTCCTAGCTT	GTTGCACCTTGAGGGGAGTC	62	385
Vin3C-4F/R	CAACAGTACGCTAACACCAGGG	GCCAGGTGATCGGGAGCC	66	253
Vin3C-12F/R	CAACAGTACGCTAACACCAGGG	TCCATGCAGCACTGGGGC	66	254
Vin3C-59F/R	CCTTTGCGCAACAGTATGCG	CTCCATGCAGCACTGGCTC	66	194
Vin3C-41F/R	GCGCAACAGTATGCGGACACG	TTGGGTCCCATGTTGCACCGT	68	341
Vin3C-49F/R	GCGCAACAGTATGCGGACACG	GTGCCACATGAACTTGCTTGG	66	307
V1C6-1F/R	CGAGCACCGCCTTCGCG	TACGCACACAAACAACCACCAAGG	62	562

The reaction systems included 2.5 µL PCR buffer, 0.2 µM of each dNTPs, 10 pmol of each primer, 2.5 units of TransTaq Hifi DNA polymerase, and 1 µg of template DNA. The conditions for PCR amplification were 94 °C for 5 min, followed by 30 cycles of 94 °C for 1 min, 58–68 °C for 30 s, 72 °C for 30 min, and a final extension of 72 °C for 7 min. PCR products were analyzed on 2% agarose gels using GelDoc XR+ with Image Lab Software.

Amplification products were purified from agarose gels with the EasyPure Quick Gel Extraction Kit. DNA amplification, cloning, and sequencing were performed at least three times for each genotype. Clones were sequenced by Huada Gene Co., Ltd (Shenzhen, China).

RNA isolation and semi-quantitative RT-PCR

Total RNA was extracted from natural mature seeds and seeds of *A. nuda* cvs HX367 at 3, 7, 14, 21, 28,

35 days post-anthesis (DPA). The root, stem, flag leaf, leaf sheath, and sterile lemma were also collected at the grain filling stage for RNA extraction. Plant samples were immediately frozen in liquid nitrogen and stored at –80 °C. TransZol Plant kit was used to extract RNA from grains, and the TransZol Up Plus RNA Kit was used to extract RNA from other tissues. A Nanodrop 2000 was used to detect the concentration and quality of RNA. RNA integrity was assessed by comparing the relative intensities of the 28S and 18S rRNA bands in 1.2% (w/v) agarose gels. cDNA was synthesized from 1 µg of the total RNA using TransScript® One-step gDNA Removal and cDNA Synthesis SuperMix (Transgen Biotech) according to the manufacturer's instructions.

Semi-quantitative RT-PCR reactions were performed in a Veriti™ 96-Well thermal cycler in a total volume of 25 µL. The reaction conditions were 94 °C for 3 min, followed by 28 cycles of 94 °C for 30 min, 56–62 °C for 30 s, 72 °C for 20 s, and a final extension

Table 2 Amino acid sequences of *AnVin-1* in *A. nuda* and *A. sativa*

	Species	Amino acid sequence			
<i>VinA1a</i>	<i>A. sativa</i>	MKTLLLLALLALAASTAFAQ ²⁰	YAQDDGWNEQGGEATGCEQQ ⁴⁰	QANLDSCKDYVTERCFTMKD ⁶⁰	FPLTWPWKWWKGGCEHEVRY ⁸⁰
<i>AnVin-1A1</i>	<i>A. nuda</i>	-----	-----	-----	-----
<i>AnVin-1A2</i>	<i>A. nuda</i>	-----	-----	-----	-----
<i>AnVin-1A3</i>	<i>A. nuda</i>	-----	-----	----- R -	-----
<i>VinC1a</i>	<i>A. sativa</i>	MKTLLLLAVLALAASTAFAQ ²⁰	YDQVDGWNEQGGEEAAGCEQQ ⁴⁰	QAKLDSCKDYVLERCFTMKD ⁶⁰	FPLTWPWKWWKGGCEHEVRY ⁶⁰
<i>AnVin-1C1</i>	<i>A. nuda</i>	-----	----- *	-----	-----
<i>AnVin-1C2</i>	<i>A. nuda</i>	-----	-----	-----	-----
<i>AnVin-1C3</i>	<i>A. nuda</i>	-----	-----	-----	-----
<i>AnVin-1C4</i>	<i>A. nuda</i>	-----	-----	-----	-----
<i>AnVin-1C5</i>	<i>A. nuda</i>	-----	----- *	-----	-----
<i>AnVin-1C6</i>	<i>A. nuda</i>	-----	-----	-----	-----
<i>AnVin-1C7</i>	<i>A. nuda</i>	-----	----- *	----- A -----	-----
<i>AnVin-1C8</i>	<i>A. nuda</i>	-----	----- *	-----	-----
<i>AnVin-1C9</i>	<i>A. nuda</i>	-----	-----	-----	----- Q -----
<i>AnVin-1C10</i>	<i>A. nuda</i>	-----	-----	-----	-----
<i>VinD1a</i>	<i>A. sativa</i>	MKTLLLLALLALAASTAFAQ ²⁰	YAQDDGWNEQGGEATGCEQQ ⁴⁰	QANLDSCKDYVMERCFTMKD ⁶⁰	FPLTWPWKWWKGGCEHKVRY ⁸⁰
<i>AnVin-1D1</i>	<i>A. nuda</i>	-----	- T ----- I -----	-----	----- E -----
<i>AnVin-1D2</i>	<i>A. nuda</i>	--- R -----	- T R ----- I -----	--- Q -----	----- E -----
<i>AnVin-1D3</i>	<i>A. nuda</i>	-----	- T ----- I -----	-----	----- E -----
<i>AnVin-1D4</i>	<i>A. nuda</i>	-----	- T ----- I -----	-----	----- E -----
<i>AnVin-1D5</i>	<i>A. nuda</i>	-----	- T ----- I -----	-----	----- E -----
<i>VinA1a</i>	<i>A. sativa</i>	QCCEQLNQVSQQCRCKAIWR	AVEHELGGFLGLQKGEIGKR ¹²⁰	LLRAKSIPSKCNMGPQCNEFP ¹⁴⁰	LTTGYYW* ¹⁴⁸
<i>AnVin-1A1</i>	<i>A. nuda</i>	-----	-----	-----	-----
<i>AnVin-1A2</i>	<i>A. nuda</i>	-----	-----	----- S -----	-----
<i>AnVin-1A3</i>	<i>A. nuda</i>	-----	-----	-----	-----
<i>VinC1a</i>	<i>A. sativa</i>	QCCEQLNQVSQQCRCKAIWR	AVEHELGGFLGLQKGEIGKR ¹²⁰	LLRAKSIPSKCNMGPQCNEFP ¹⁴⁰	LTTGYYW* ¹⁴⁸
<i>AnVin-1C1</i>	<i>A. nuda</i>	-----	--- R ----- Q S -----	M ----- A -----	-----
<i>AnVin-1C2</i>	<i>A. nuda</i>	-----	--- R ----- Q S -----	M ----- A ----- R ---	-----
<i>AnVin-1C3</i>	<i>A. nuda</i>	-----	--- R ----- Q S -----	M ----- A -----	-----
<i>AnVin-1C4</i>	<i>A. nuda</i>	-----	--- R ----- Q S -----	M ----- A -----	-----
<i>AnVin-1C5</i>	<i>A. nuda</i>	-----	--- R ----- Q S -----	M ----- A -----	-----
<i>AnVin-1C6</i>	<i>A. nuda</i>	-----	----- Q S -----	M ----- A -----	-----
<i>AnVin-1C7</i>	<i>A. nuda</i>	-----	--- R ----- Q S -----	M ----- A -----	-----
<i>AnVin-1C8</i>	<i>A. nuda</i>	-----	--- R ----- Q S -----	M ----- A - * D -----	-----
<i>AnVin-1C9</i>	<i>A. nuda</i>	-----	--- R ----- Q S -----	M ----- A -----	-----
<i>AnVin-1C10</i>	<i>A. nuda</i>	-----	--- R ----- Q S -----	M ----- A -----	-----
<i>VinD1a</i>	<i>A. sativa</i>	QCCEQLNQVSQQCRCKAI	AVEHELGGFLGLQKGEIGKH	LLRAKSIPSKCNMGPQCNEF	LTTGYYW* ¹⁴⁸
<i>AnVin-</i>	<i>A. nuda</i>	-----	----- R -----	-----	-----
<i>AnVin-</i>	<i>A. nuda</i>	-----	----- R -----	-----	-----
<i>AnVin-</i>	<i>A. nuda</i>	-----	----- R -----	-----	-----
<i>AnVin-</i>	<i>A. nuda</i>	----- *	----- R -----	----- D -----	-----
<i>AnVin-</i>	<i>A. nuda</i>	-----	----- R -----	-----	-----

of 72 °C for 7 min. Values were normalized to the amplification rate of the actin gene as a constitutively expressed internal control (Tao et al. 2013). The

RT-PCR products were separated on a 2.0% agarose gel. Three replicates were performed for each sample.

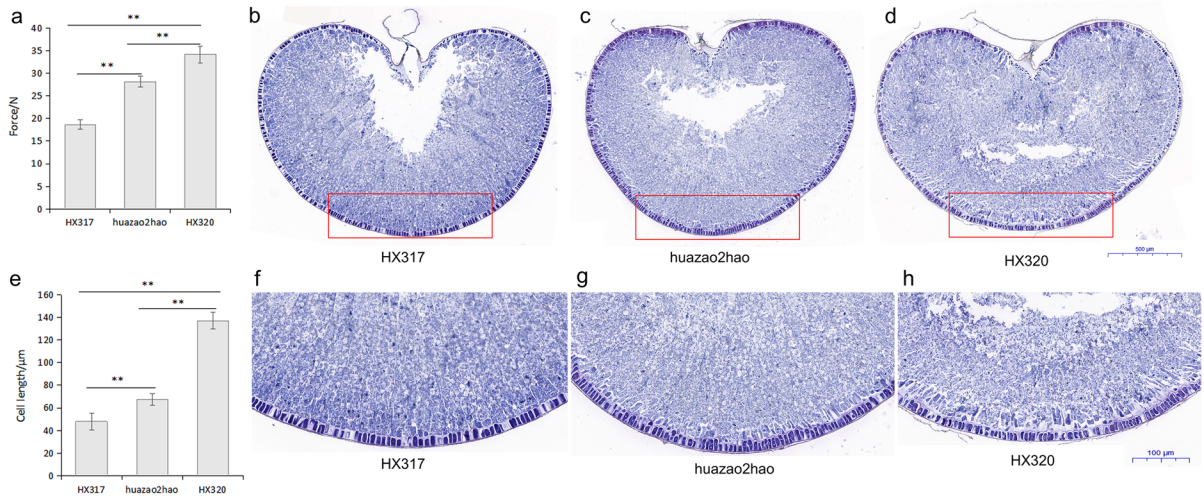


Fig. 1 Kernel hardness and paraffin sections. **a** Measure of kernel hardness for HX317, huazao2hao, and HX320. Results are presented as mean and SD; $n=100$. $**p<0.01$. **b–d** Paraffin section of mature grains in cross-section of HX317, huazao2hao and HX320. Aleurone layer and part of the inner endosperm of the kernel (red frame). Bar, 500 μm . The mag-

nification levels of **b–d** are 3.3x. **e** Cell length of the subaleurone layer for HX317, huazao2hao, and HX320. Results are presented as mean and SD; $n=6$. $**p<0.01$. **f–h** Magnified view of the aleurone layer and part of the inner endosperm of HX317, huazao2hao and HX320. The magnification levels of **f–h** are 10x. Bar, 100 μm

Sequence alignment and bioinformatics analysis

The sequence analysis of the *Vin* genes was performed in the genome database of OT3098 published on the GrainGenes website at https://wheat.pw.usda.gov/GG3/graingenes_downloads/oat-ot3098-pepsico. Protein secondary and tertiary structures were predicted using the online website at https://npsa-prabi.ibcp.fr/cgi-bin/npsa_automat.pl?page=npsa_sopma.html and <https://swissmodel.expasy.org/interactive>. *Vin* sequences of diploid, tetraploid, hexaploid oats, wheat, barley, and triticale were downloaded from the NCBI Nucleotide database. MEGA 7 was used to construct the Neighbor-joining evolutionary tree with a bootstrap value at 1000 replicates.

Development of CAPS marker

DNAMAN software was used to compare and analyze the sequences of the sequencing results. The sequence files were submitted to Dna SP v.5.0 for extraction of variant sites, and haplotype analysis was performed on all variant sites. DNAMAN software was used to analyze whether there was a suitable restriction site near the SNP position of the sequence. Restriction endonucleases can recognize the difference of a single

base, and the polymorphism of the restriction site can be used to establish the target. According to previous studies, specific primers of V1C6 gene were designed and synthesized (Table 2). PCR reactions were performed in a Veriti™ 96-Well Thermal Cycler in a total volume of 25 μL . The reaction systems included 2.5 μL PCR buffer, 0.2 μM of each dNTPs, 10 pmol of each primer, 2.5 units of TransTaq Hifi DNA polymerase, and 1 μg of template DNA. The conditions for PCR amplification were 94 $^{\circ}\text{C}$ for 5 min, followed by 30 cycles of 94 $^{\circ}\text{C}$ for 1 min, 62 $^{\circ}\text{C}$ for 30 s, 72 $^{\circ}\text{C}$ for 30 min, and a final extension of 72 $^{\circ}\text{C}$ for 7 min. Enzyme digestion reaction were performed in a *Fly-Cut*® EcoRI in a total volume of 20 μL . The reaction systems included 1 μg PCR product, 2 μL 10 \times *Fly-Cut*® Buffer 0.5 μL FlyCut® EcoRI and corresponding Nuclease-free Water. The conditions for enzyme digestion reaction was 37 $^{\circ}\text{C}$ for 15 min in metal bath. The digested products were detected by 2% agarose gel electrophoresis.

Subcellular localization

The *AnVin-1C6* and *AnVin-3C2* genes were fused with green and red fluorescent protein genes, respectively, to make the recombinant expression

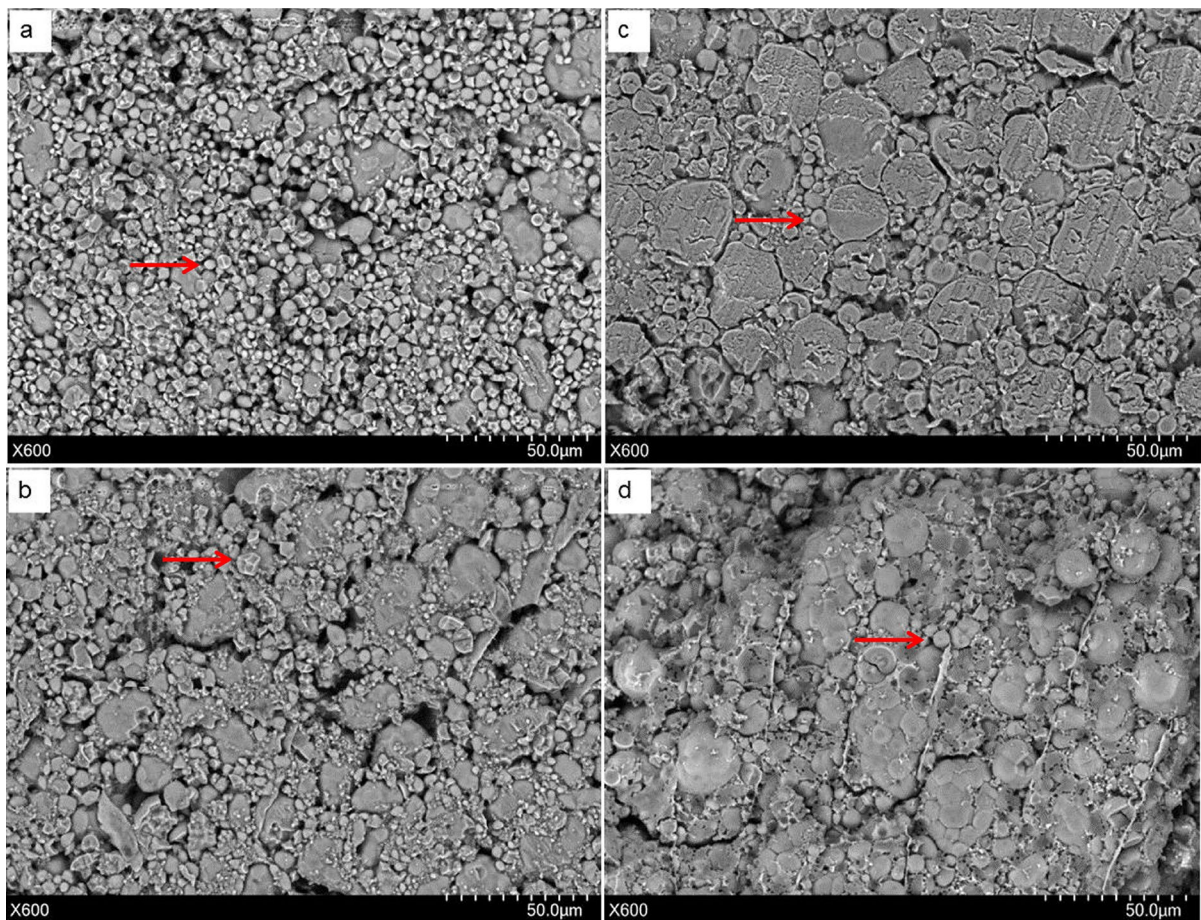
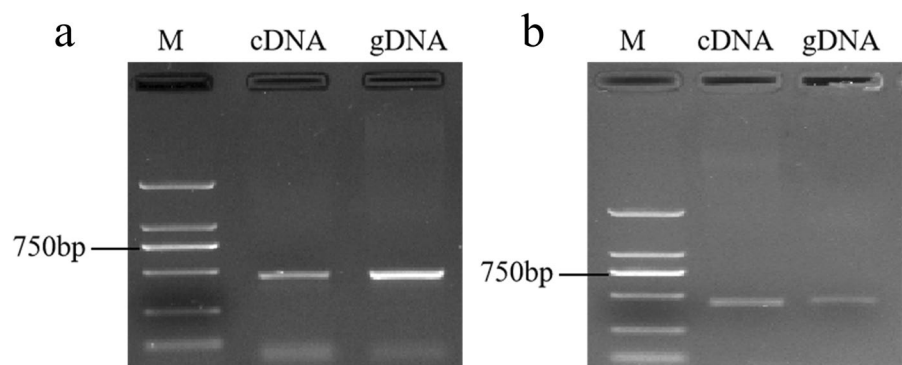


Fig. 2 SEM images of naked oat endosperm. **a** The internal endosperm structure of HX317. **b** The subaleurone layer endosperm structure of HX317. **c** The internal endosperm

structure of HX320. **d** The subaleurone layer endosperm structure of HX320. Bar, 50 μ m. The red arrows point to the starch granule

Fig. 3 Cloning of *AnVin-1* and *AnVin-3* genes from HX367 **a** Amplification of *AnVin-1* gene on cDNA and DNA. M, 2 K marker. **b** Amplification of *AnVin-3* gene on cDNA and DNA. M, 2 K marker



vectors pBWA(V)HS-V1C6-GLosgfp and pBWA(V)HS-V3C2-mKATE. The recombinant vectors were transformed into *Agrobacterium* GV3101 by

electroporation. An empty vector was used as a control. Tobacco plants were injected at the lower epidermis of the leaves with a one mL syringe with the

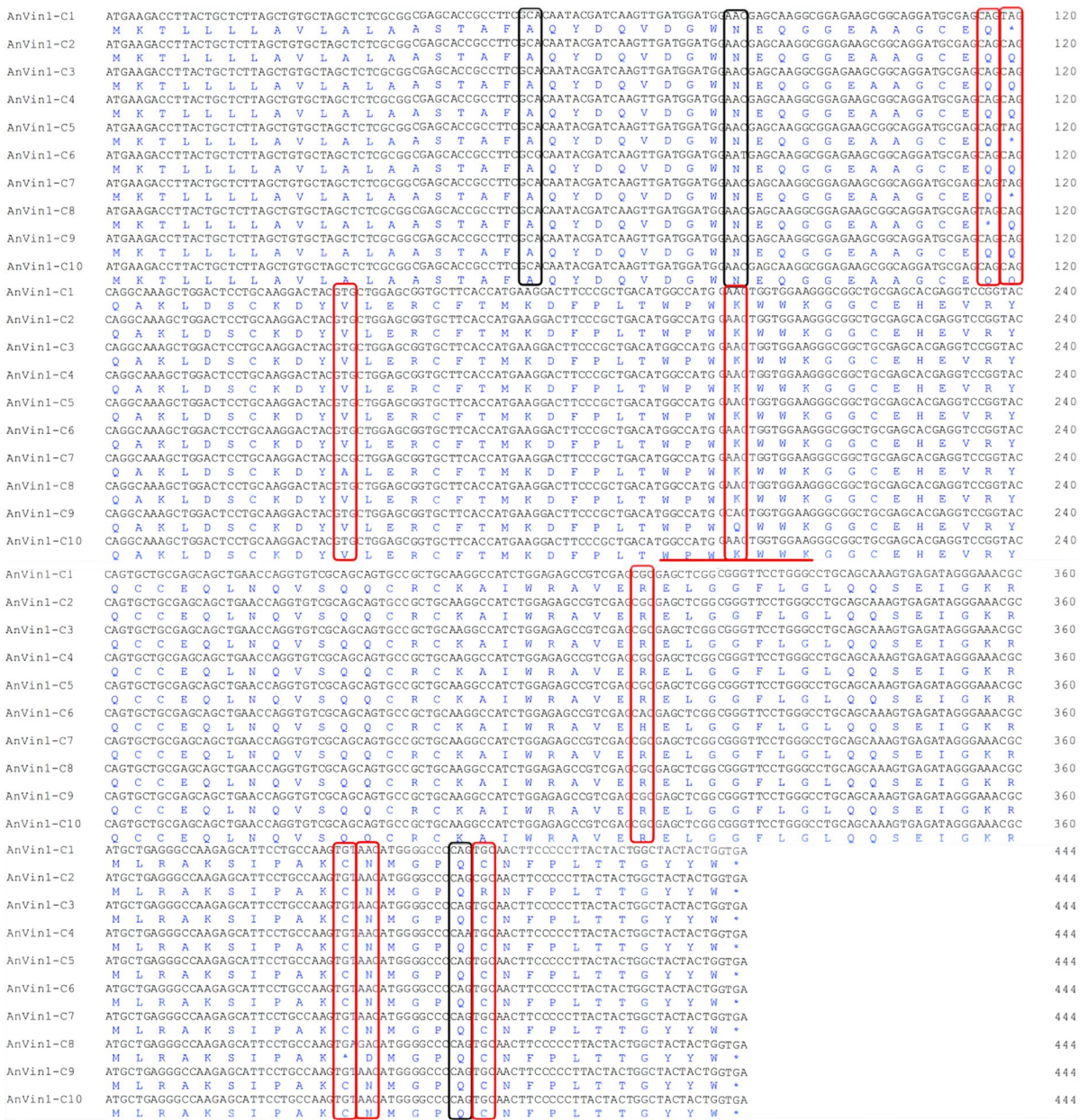


Fig. 4 Sequence alignment of the *AnVin-1C* gene and amino acids. Black boxes indicate synonymous mutations or nonsynonymous mutations, red boxes indicate missense mutations. The red line indicates the conserved domain

tip removed and marked. The injected tobacco plants were cultured in low light for two days. The marked tobacco leaves were mounted onto glass slides, observed under a laser confocal microscope, and photographed.

Statistical analysis

One-Way ANOVA in SPSS 21.0 software was used to conduct one-way analysis of variance on the experimental data and LSD method was used to conduct multiple comparisons to analyze the correlation between different haplotypes and oat kernel hardness.

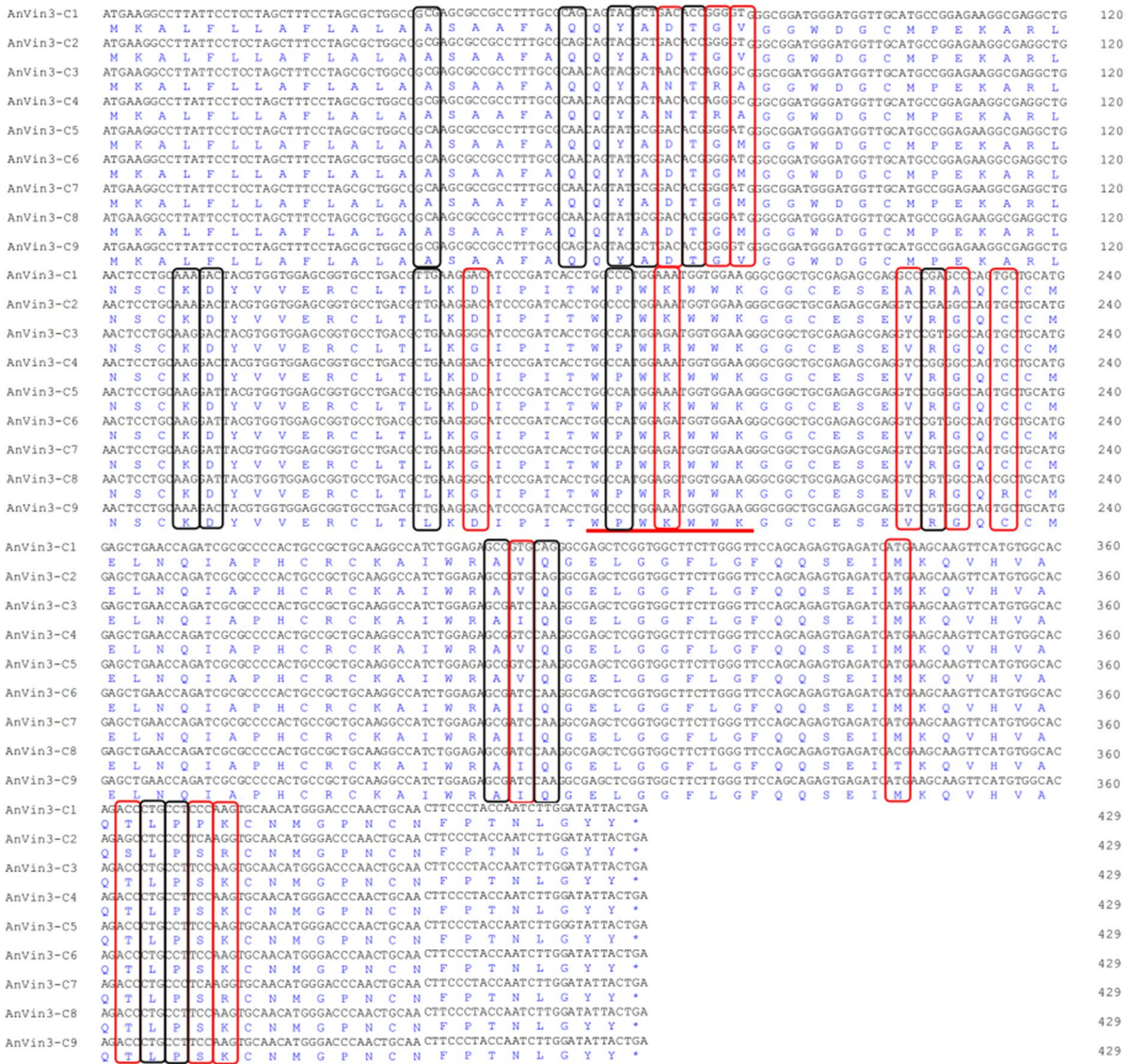


Fig. 5 Sequence alignment of the *AnVin-3C* gene and amino acids. Black boxes indicate synonymous mutations or nonsense mutations, red boxes indicate missense mutations. The red line indicates the conserved domain

Results

Cellular structure of grains with different hardness values in *Avena sativa*

The hardness values for HX317 (soft), huazao2hao (medium), and HX320 (hard) were determined by TA, and they were significantly different (Fig. 1a). Paraffin sections showed that the internal structure of *A. nuda* was composed of a seed coat, pericarp, aleurone

layer, subaleurone layer, and starchy endosperm. The aleurone layer in each oat was composed of a single layer of cells of similar cell sizes. The structure difference of kernels with different hardness was manifested in the sub-aleurone layer and the inner floury endosperm. The sub-aleurone layer of soft oats is not obvious. The cell length was $47.8 \mu\text{m} \pm 7.6$, and even the secondary powder layer is missing in some parts. The sub-aleurone layer of hard oat had a distinct structure, with long cells obvious structure and

Table 3 Amino acid sequences of *AnVin-3* in *A. nuda* and *A. sativa*

Gene	species	Amino acid sequence			
<i>VinC3a</i>	<i>A. sativa</i>	MKALFLLAFLALAASAAFAQ ²⁰	QYANTRAGGWDCMPEKARL ⁴⁰	NSCKDYVVERCLTLK ^{DIPIT} ⁶⁰	WPWK ^{WWKGGCESEVR} ^{GQCCM} ⁸⁰
<i>VinC3b</i>	<i>A. sativa</i>	-----	---D-GM-----	-----G---	---R-----
<i>AnVin-3C1</i>	<i>A. nuda</i>	-----	---D-GV-----	-----D---	---K-----A-A---
<i>AnVin-3C2</i>	<i>A. nuda</i>	-----	---D-GV-----	-----D---	---K-----
<i>AnVin-3C3</i>	<i>A. nuda</i>	-----	---N-RA-----	-----G---	---R-----
<i>AnVin-3C4</i>	<i>A. nuda</i>	-----	---N-RA-----	-----D---	---K-----
<i>AnVin-3C5</i>	<i>A. nuda</i>	-----	---D-GM-----	-----D---	---K-----
<i>AnVin-3C6</i>	<i>A. nuda</i>	-----	---D-GM-----	-----G---	---R-----
<i>AnVin-3C7</i>	<i>A. nuda</i>	-----	---D-GM-----	-----G---	---R-----
<i>AnVin-3C8</i>	<i>A. nuda</i>	-----	---D-GM-----	-----G---	---R-----R---
<i>AnVin-3C9</i>	<i>A. nuda</i>	-----	---D-GV-----	-----D---	---K-----
<i>VinC3a</i>	<i>A. sativa</i>	ELNQIAPHCRCKAIWRAVQ ¹⁰⁰	ELGGFLGFQQ SEIMKQVHVA ¹²⁰	QTLPSK ^{CNMGPNCFPTNLG} ¹⁴	YY* ¹⁴³
<i>VinC3b</i>	<i>A. sativa</i>	-----I--	-----	-----	---
<i>AnVin-3C1</i>	<i>A. nuda</i>	-----V--	-----	-----	---
<i>AnVin-3C2</i>	<i>A. nuda</i>	-----V--	-----	-S---R-----	---
<i>AnVin-3C3</i>	<i>A. nuda</i>	-----I--	-----	-----	---
<i>AnVin-3C4</i>	<i>A. nuda</i>	-----V--	-----	-----	---
<i>AnVin-3C6</i>	<i>A. nuda</i>	-----I--	-----	-----	---
<i>AnVin-3C7</i>	<i>A. nuda</i>	-----I--	-----	-----R-----	---
<i>AnVin-3C8</i>	<i>A. nuda</i>	-----I--	-----T-----	-----	---
<i>AnVin-3C9</i>	<i>A. nuda</i>	-----I--	-----	-----	---

long cells (137.3 μm ± 7.3) inserted into the intercellular spaces of the endosperm. Endosperm cells of soft oat were arranged neatly and loosely, while those of hard oat were more closely arranged. The aleurone cells and endosperm cells of HX317 kernels were well-ordered. The arrangement of the aleurone cells became more disordered with increased kernel hardness value.

Ultrastructure of the endosperm of naked oats with different hardness.

SEM of the endosperm structures of HX317 and HX320 kernels was performed. The structures of the central endosperm and subaleurone layers of HX317 were loose with large gaps (Fig. 2a and b). Starch granules were primarily in the form of single and small grains (Fig. 2a). The structures of the central endosperm and subaleurone layers of HX320 were compact with small gaps (Fig. 2c and d). The starch granules were large and tightly bound to the surrounding protein matrix (Fig. 2c). The structure of the subaleurone layer of HX320 near the grain cortex was also more compact than that of HX317 (Fig. 2b and d).

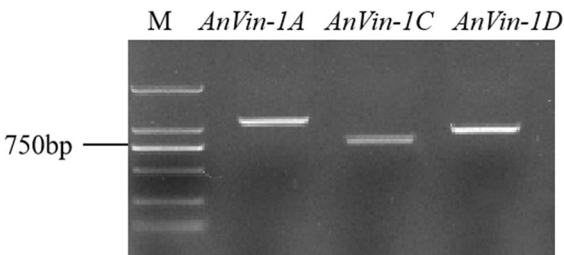


Fig. 6 Genetic markers of *AnVin-1* on A, C, and D genomes. The fragment sizes of *AnVin-1A*, *AnVin-1C*, and *AnVin-1D* were 1082 bp, 754 bp, and 872 bp, respectively

Isolation and sequence analysis of *AnVin-1* and *AnVin-3* genes in *Avena nuda* L.

Genomic DNA and cDNA from HX367 were amplified using primer pairs *Vin-1F/R* and *Vin-3F/R* (Table 1). The sizes of the amplified *AnVin-1* and *AnVin-3* products at the gDNA and cDNA levels

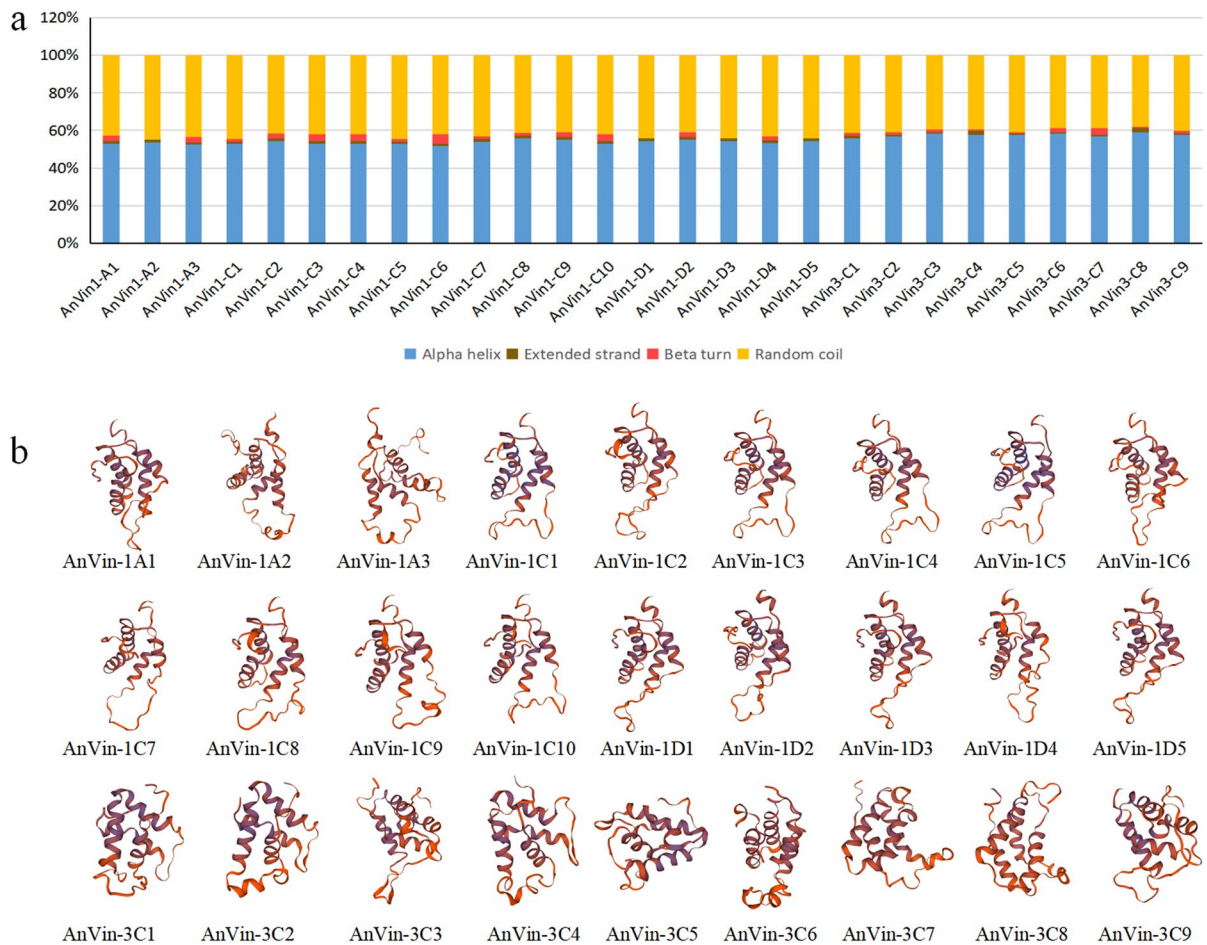


Fig. 7 The secondary (a) and tertiary (b) structures of the AnVin-1 and AnVin-3 proteins

were the same (Fig. 3), indicating that these genes in *A.nuda* included a single complete ORF with no introns. Multiple sequence alignment analysis showed that the *AnVin-1* and *AnVin-3* genes of naked oats existed as multiple copies. The multiple sequences of *AnVin-1* were named *AnVin-1A1*, *AnVin-1A2*, *AnVin-1A3*, *AnVin-1C1*, *AnVin-1C2*, *AnVin-1C3*, *AnVin-1C4*, *AnVin-1C5*, *AnVin-1C6*, *AnVin-1C7*, *AnVin-1C8*, *AnVin-1C9*, *AnVin-1C10*, *AnVin-1D1*, *AnVin-1D2*, *AnVin-1D3*, *AnVin-1D4*, and *AnVin-1D5*. The multiple sequences of *AnVin-3* were named *AnVin-3C1*, *AnVin-3C2*, *AnVin-3C3*, *AnVin-3C4*, *AnVin-3C5*, *AnVin-3C6*, *AnVin-3C7*, *AnVin-3C8*, and *AnVin-3C9*.

Multiple sequence alignment analysis showed that the homology among the *AnVin-1* genes ranged from 96.13 to 99.77%, and the homology of *AnVin-3*

genes ranged from 94.17 to 99.30%. The multi-copy sequences showed single base pair differences. There were 3 SNPs in *AnVin-1A*, resulting in 2 missense mutations and 1 synonymous mutation (Supplementary file 2, Table 2). There were 8 SNPs in *AnVin-1D*, resulting in 5 missense mutations and 3 synonymous mutations (Supplementary file 3, Table 2). There were 11 SNPs in *AnVin-1C*, resulting in 4 synonymous mutations, 4 missense mutations, and 5 non-sense mutations. One of the missense mutations in *AnVin-1C* (K/Q) occurred in the tryptophan-rich region of “WPWKWWK” (Fig. 4, Table 2). There were 32 SNPs in *AnVin-3C*, resulting in 15 synonymous mutations, 17 missense mutations, and one nonsense mutation. One of the missense mutations in *AnVin-3C* (K/R) also occurred in the “WPWKWWK” region (Fig. 5, Table 3).

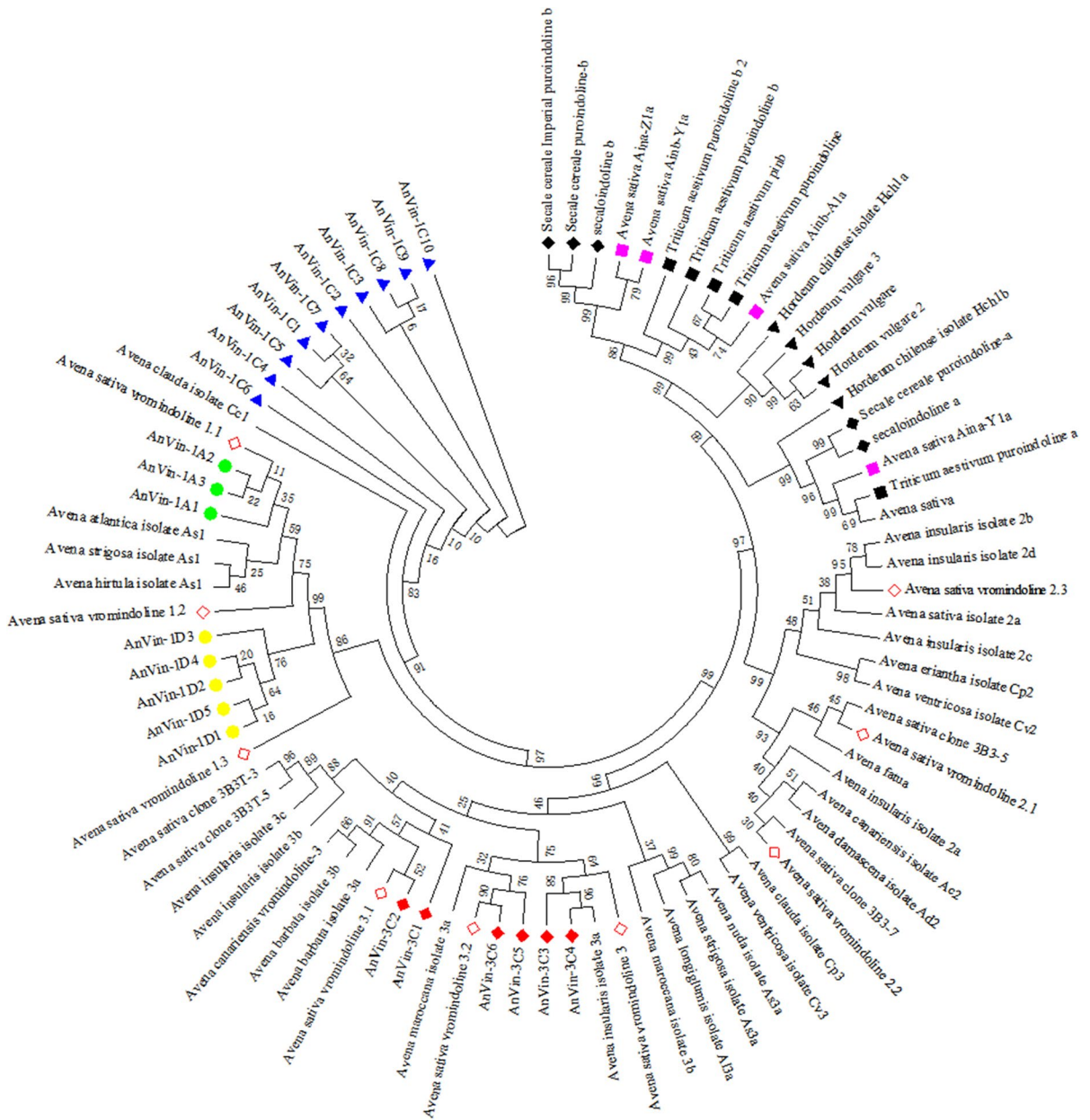


Fig. 8 Phylogenetic analysis of *AnVin-1*, *AnVin-3* *Vin*-like genes in *Avena* and related species. The green circles represent the *AnVin-1A* genes; the yellow circles represent the *AnVin-1D* genes; the blue triangles represent the *AnVin-1C* genes; and the red diamonds represent *AnVin-3C*. The purple squares and

red line diamonds represent the *Vin* and *Ain* gene in *A. sativa*. Black squares represent the *Pin* genes in wheat; black triangles represent the *Hin* genes in barley; and black diamonds represent the *Sin* genes in triticale

The amino acid sequence similarity of between *VinA1a* in *A. sativa* and *AnVin-1A1* in *A. nuda* was 100%. *VinA1a* differed from *AnVin-1A2* and *AnVin-1A3* by one amino acid each (Table 2). Compared

with *VinC1a* in *A. sativa*, *AnVin-1C* had 5 amino acids that were unique to *A. nuda*. Similarly, *AnVin-1D* had 3 unique amino acids (Table 2). *VinC3a* in *A. sativa* has 2 isoforms containing 6 amino acid

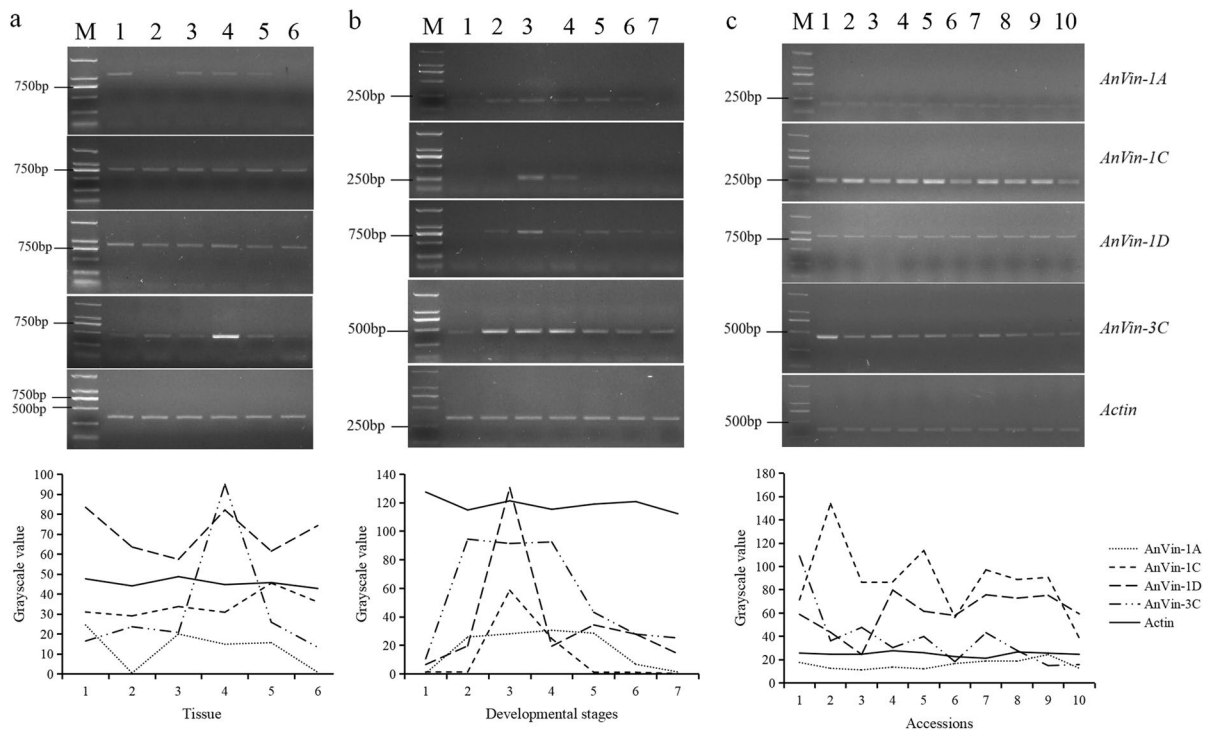


Fig. 9 The expression pattern of *AnVin-1* and *AnVin-3*. **a** Expression in different tissues. Lanes 1–6 represent roots, stems, flag leaves, leaf sheaths, protective glumes, and mature grains, respectively. **b** Expression at different developmental stages. Lanes 1–7 represent 3, 7, 14, 21, 28, and 35 DAP and

mature grains after flowering, respectively. **c** Expression in 14 DAP kernels of different hardness values, lanes 1–10 represent HX317, HX88, HX106, HX54, HX344, HX310, HX268, HX21, HX265, and HX320, respectively

differences (Table 3). The 9 sequences of *AnVin-3C* in *A.nuda* contain this 6 amino acid, while the 27th amino acid in the coding region is a specific amino acid for *A.nuda* (Table 3).

Genomic marker development of *AnVin-1* gene in *Avena nuda* L.

The upstream and downstream 500 bp sequences of *AnVin-1A*, *AnVin-1C*, and *AnVin-1D* coding sequences were obtained from the predicted sequence of *AnVin-1* in the OT3098 database. (Supplementary file 4). Primers were designed based on the specific site of *AnVin-1* between three genomes. PCR amplification was performed on HX367 gDNA using the primers *Vin-1A1F/R*, *Vin-1C1F/R*, and *Vin-1D1F/R* (Table 1, Fig. 6).

Bioinformatics analysis of *AnVIN-1* and *AnVIN-3* proteins of *Avena nuda* L.

AnVIN-1 and *AnVIN-3* were found to be 147 and 142 amino acids long, respectively. Both proteins included a “WPWKWWK” tryptophan-rich region and 10 cysteines. Conserved domain searching revealed that *AnVIN-1* and *AnVIN-3* belonged to the seed storage protein (SS) subfamily of the alpha-amylase inhibitors (AAIs) superfamily. The predicted secondary structures of *AnVIN-1* and *AnVIN-3* contained α helices, β sheets, random coils, and extended strands (Fig. 7a). The predicted tertiary structures of *AnVIN-1* based on the A, C, and D genomes were similar, but there were differences in the tertiary structure of *AnVIN-1* and *AnVIN-3* proteins (Fig. 7b).

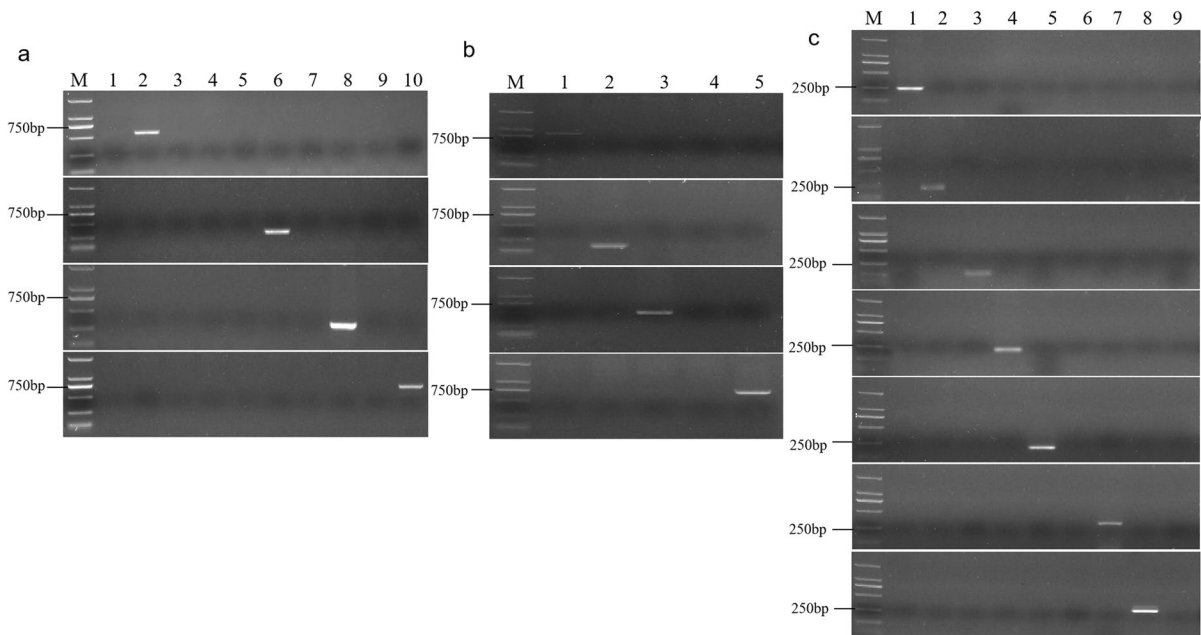


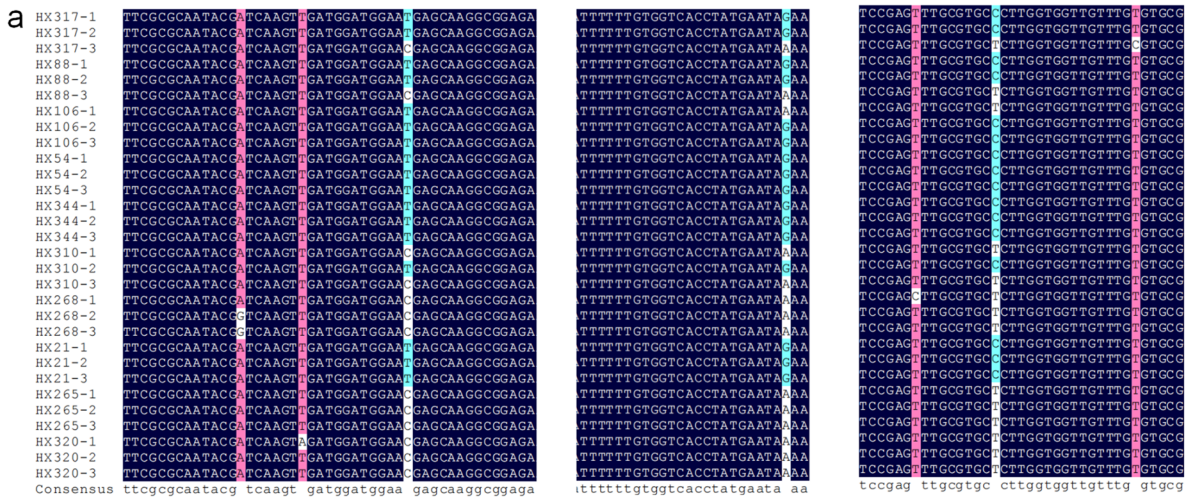
Fig. 10 Identification of single copy sequence of *AnVin-1* and *AnVin-3*. **a** Different copy sequence identification of *AnVin-1C*. Lanes 1–10 represent *AnVin-1C1* to *AnVin-1C10* sequences. **b** Different copy sequence identification of *AnVin-*

1D. Lanes 1–5 represent *AnVin-1D1* to *AnVin-1D5* sequences. **c** Different copy sequence identification of *AnVin-3C*. Lanes 1–9 represent *AnVin-3C1* to *AnVin-3C9* sequences

A phylogenetic tree was constructed with *Vin-like* gene sequences in diploid, tetraploid, hexaploid of oat, and wheat, barley, and triticale. The analysis showed that multiple distinct copies of each of the *AnVin-1A*, *AnVin-1C*, *AnVin-1D*, and *AnVin-3C* gene sequences clustered together. *AnVin-1A*, *AnVin-1C*, and *AnVin-3C* were clustered with diploid A and C genomes, respectively. *AnVin-1A* and *AnVin-1D* genes were clustered together in the same branch, indicating that they were more closely related. *AnVin-1* and *AnVin-3* genes were on different branches, indicating that they represented two different *AnVin* genes (Fig. 8). The *AnVin* genes were more closely related to their counterparts in other species of the oat genus than the more distantly related wheat, barley, and triticale (Fig. 8). In addition, the *Ain* gene in *A. sativa* was more closely related to the *Pin*, *Hin* and *Sin* genes in wheat, barley, and triticale than to the *AnVin* gene in *A. nuda* (Fig. 8).

Expression pattern of *AnVin-1* and *AnVin-3* in *Avena nuda* L.

Semi-quantitative RT-PCR analyses among different tissues of oat showed that *AnVin-1C*, *AnVin-1D*, and *AnVin-3C* were expressed in all tested tissues (Fig. 9). However, *AnVin-1A* was not expressed in stems and mature kernels (Fig. 9a). The expression of *AnVin-3C* was the highest in leaf sheaths (Fig. 9a). The expression levels of *AnVin-1* and *AnVin-3* first increased and then decreased at different stages of grain development, with the highest expression levels at 14 DAP (Fig. 9b). From the 260 oats, 5 extremely soft and 5 extremely hard materials were selected for hardness measurements and differential gene expression analysis. The results showed that there was little difference in the expression levels of *AnVin-1A* and *AnVin-1D* in kernels at 14 DAP among the 10 materials. However, the expression levels of *AnVin-1C* and *AnVin-3C* in soft oat were higher than those in hard oat (Fig. 9c).



b

Effect	exon	3' UTR			No. of accessions
Position	153	598	648		
Hap1	T	G	C	16	
Hap2	T	A	T	1	
Hap3	C	A	T	13	

Fig. 11 Sequence alignment and haplotypes of full-length of *AnVin-1C6* in 10 materials with different hardness values. Positions 153, 598, and 648 are the sites of allelic variation. The full-length sequences are shown in Supplementary file 5



b

Effect	exon		No. of accessions
Position	207	291	
Hap1	T	T	20
Hap2	C	C	7
Hap3	C	G	3

Fig. 12 Sequence alignment and haplotypes of the coding region of *AnVin-3C2* in 10 materials with different hardness values. Positions 207 and 291 are the sites of allelic variation. The coding region sequences are shown in Supplementary file 6

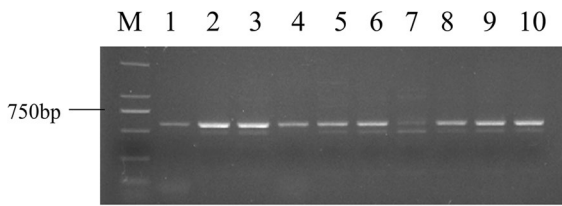


Fig. 13 Gel electrophoresis of 10 materials of *AnVin-1C6* gene sequence digested by *EcoRI*. Lanes 1–10 represent HX320, HX265, HX21, HX268, HX310, HX344, HX54, HX106, HX88, and HX317

Gene markers development for different copy sequences of *AnVin-1* and *AnVin-3*

Due to the high sequence similarity of the three *AnVin-1A* sequences, no specific primer could be designed for single-copy sequences. The primers were designed based on specific sites in the 10 *AnVin-1C* sequences. The primers Vin1C-133F/R, Vin1C-3F/R, Vin1C-94F/R, and Vin1C-101F/R were used to obtain the sequences of *AnVin-1C2*, *AnVin-1C6*, *AnVin-1C8*, and *AnVin-1C10*, respectively (Fig. 10a). The primers Vin1D-9F/R, Vin1D-17F/R, Vin1D-56F/R, and Vin1D-29F/R were used to obtain the sequences of *AnVin-1D1*, *AnVin-1D2*, *AnVin-1D3*, and *AnVin-1D5*, respectively (Fig. 11b). The primers Vin3C-16F/R, Vin3C-26F/R, Vin3C-4F/R, Vin3C-12F/R, Vin3C-59F/R, Vin3C-41F/R, and Vin3C-49F/R were used to obtain the sequences of *AnVin-3C1*, *AnVin-3C2*, *AnVin-3C3*, *AnVin-3C4*, *AnVin-3C5*, *AnVin-3C7*, and *AnVin-3C8*, respectively (Fig. 11c). These primers were the gene markers of the sequences of *AnVin-1* and *AnVin-3*.

Haplotype analysis of *AnVin-1* and *AnVin-3* genes in naked oats

Specific primers were used for the identification of copy sequences in the 5 extremely soft and 5 extremely hard materials (Table 1, Fig. 10). Only *AnVin-1C6*, *AnVin-1C8*, *AnVin-1D2*, *AnVin-1D3*, *AnVin-3C2*, and *AnVin-3C4* could be identified in the 10 materials. The other sequences appeared in only individual materials. Among the sequences, only *AnVin-1C6* and *AnVin-3C2* had three haplotypes in the 10 materials, which had polymorphisms at 153 bp (T/C), 598 bp (G/A), and 648 bp (C/T), respectively,

and these changes were linked. The polymorphism at 153 bp was located in the coding region but did not cause a change in the amino acid sequence. The other two polymorphisms were located in the 3'-UTR region (Fig. 11, Supplementary file 5). There were three haplotypes of *AnVin-3C2* in the 10 materials, with linked changes at 207 and 291 bp (Fig. 12, Supplementary file 6). The SNP at 207 bp was a synonymous mutation, while the SNP at 291 bp caused a missense mutation (Cys to Arg).

Development and validation of molecular markers for grain hardness in *Avena nuda* L.

An *EcoRI* cleavage site was found at site 598 bp of *AnVin-1C6*. Amplified samples from the 10 materials were digested with *EcoRI*. The haplotype resistant to *EcoRI* digestion was named *AnVin-1C6b*, while the haplotype that could be digested into two fragments was named *AnVin-1C6a* (Fig. 13). The amplified fragments of 56 softest and 56 hardest naked oats were digested with *EcoRI* (Table 4). Among the 112 tested naked oats, 79.5% (89/112) were of the *AnVin-1C6a* genotype, and 20.5% (23/112) were of the *AnVin-1C6b* genotype. The average hardness values of the 56 soft and hard oats were 26.69 and 28.23 N, respectively. Correlation analysis and one-way ANOVA showed that the hardness values of the two genotypes had a low correlation ($R=0.120$), and the difference was not significant ($P=0.207$). The sum of squared deviations between groups accounted for 1.44% of the total sum of squared deviations (Table 5). The results showed that the CAPS marker had a very low interpretation of the hardness variation in these 112 natural populations.

Subcellular localization of *AnVin-1C6* and *AnVin-3C2* genes

AnVin-1C6 and *AnVin-3C2* were fused to the N-termini of green and red fluorescent protein genes, respectively, to construct fusion expression vectors (Supplementary file 7). These vectors were transformed into tobacco leaf cells. The green fluorescence of *AnVin-1C6* and the red fluorescence of *AnVin-3C2* may be concentrated in cytomembrane (Fig. 14). The expression effect of both genes is weak.

Table 4 CAPS marker verification of 112 naked Oat natural population materials

Num.	Code	Source	Hardness value/N	AnVin1-C6 allele type	Num.	Code	Source	Hardness value/N	AnVin1-C6 allele type
1	HX109	YunNan	17.72	<i>AnVin1-C6a</i>	57	HX320	ShanXi	37.26	<i>AnVin1-C6b</i>
2	HX111	SiChuan	18.15	<i>AnVin1-C6a</i>	58	HX265	Inner Mongolia	36.05	<i>AnVin1-C6a</i>
3	HX317	ShanXi	18.62	<i>AnVin1-C6a</i>	59	HX21	HeBei	35.47	<i>AnVin1-C6a</i>
4	HX349	ShanXi	19.26	<i>AnVin1-C6a</i>	60	HX268	Inner Mongolia	35.03	<i>AnVin1-C6b</i>
5	HX110	SiChuan	19.29	<i>AnVin1-C6a</i>	61	HX256	HeBei	35.01	<i>AnVin1-C6a</i>
6	HX97	GuiZhou	19.37	<i>AnVin1-C6a</i>	62	HX310	ShanXi	34.69	<i>AnVin1-C6a</i>
7	HX88	ShanXi	20.08	<i>AnVin1-C6a</i>	63	HX136	Russia	34.12	<i>AnVin1-C6a</i>
8	HX91	ShanXi	20.69	<i>AnVin1-C6a</i>	64	HX254	HeBei	33.94	<i>AnVin1-C6a</i>
9	HX113	SiChuan	20.79	<i>AnVin1-C6a</i>	65	HX263	Inner Mongolia	33.84	<i>AnVin1-C6a</i>
10	HX337	ShanXi	21.04	<i>AnVin1-C6a</i>	66	HX142	France	33.68	<i>AnVin1-C6a</i>
11	HX338	ShanXi	21.39	<i>AnVin1-C6a</i>	67	HX321	ShanXi	33.51	<i>AnVin1-C6a</i>
12	HX261	Inner Mongolia	21.40	<i>AnVin1-C6a</i>	68	HX120	Canada	33.10	<i>AnVin1-C6a</i>
13	HX106	YunNan	21.62	<i>AnVin1-C6b</i>	69	HX140	Hungary	33.08	<i>AnVin1-C6a</i>
14	HX54	ShanXi	21.70	<i>AnVin1-C6a</i>	70	HX40	Inner Mongolia	32.83	<i>AnVin1-C6a</i>
15	HX52	ShanXi	21.72	<i>AnVin1-C6a</i>	71	HX296	Inner Mongolia	32.80	<i>AnVin1-C6a</i>
16	HX333	ShanXi	21.81	<i>AnVin1-C6a</i>	72	HX18	HeBei	32.76	<i>AnVin1-C6a</i>
17	HX344	ShanXi	21.89	<i>AnVin1-C6a</i>	73	HX139	Hungary	32.73	<i>AnVin1-C6a</i>
18	HX302	Russia	22.01	<i>AnVin1-C6a</i>	74	HX299	Inner Mongolia	32.63	<i>AnVin1-C6b</i>
19	HX55	ShanXi	22.03	<i>AnVin1-C6a</i>	75	HX255	HeBei	32.59	<i>AnVin1-C6b</i>
20	HX56	ShanXi	22.08	<i>AnVin1-C6a</i>	76	HX371	Chile	32.52	<i>AnVin1-C6b</i>
21	HX96	GuiZhou	22.10	<i>AnVin1-C6a</i>	77	HX45	Inner Mongolia	32.27	<i>AnVin1-C6b</i>
22	HX43	Inner Mongolia	22.10	<i>AnVin1-C6b</i>	78	HX370	Chile	32.16	<i>AnVin1-C6b</i>
23	HX53	ShanXi	22.13	<i>AnVin1-C6a</i>	79	HX274	Inner Mongolia	32.08	<i>AnVin1-C6b</i>
24	HX84	ShanXi	22.14	<i>AnVin1-C6b</i>	80	HX39	Inner Mongolia	32.07	<i>AnVin1-C6a</i>
25	HX42	Inner Mongolia	22.16	<i>AnVin1-C6a</i>	81	HX67	ShanXi	32.02	<i>AnVin1-C6a</i>
26	HX103	YunNan	22.17	<i>AnVin1-C6a</i>	82	HX138	Hungary	31.98	<i>AnVin1-C6b</i>
27	HX105	YunNan	22.34	<i>AnVin1-C6a</i>	83	HX292	Hungary	31.93	<i>AnVin1-C6a</i>
28	HX116	SiChuan	22.37	<i>AnVin1-C6a</i>	84	HX253	HeBei	31.93	<i>AnVin1-C6b</i>
29	HX343	ShanXi	22.37	<i>AnVin1-C6a</i>	85	HX115	SiChuan	31.91	<i>AnVin1-C6a</i>
30	HX289	Russia	22.42	<i>AnVin1-C6a</i>	86	HX354	ShanXi	31.85	<i>AnVin1-C6a</i>
31	HX51	ShanXi	22.55	<i>AnVin1-C6a</i>	87	HX61	ShanXi	31.52	<i>AnVin1-C6a</i>
32	HX328	ShanXi	22.64	<i>AnVin1-C6a</i>	88	HX37	Inner Mongolia	31.43	<i>AnVin1-C6a</i>
33	HX367	ShanXi	22.67	<i>AnVin1-C6a</i>	89	HX141	Hungary	31.35	<i>AnVin1-C6a</i>
34	HX327	ShanXi	22.69	<i>AnVin1-C6a</i>	90	HX319	ShanXi	31.24	<i>AnVin1-C6a</i>
35	HX318	ShanXi	22.78	<i>AnVin1-C6b</i>	91	HX99	GuiZhou	31.08	<i>AnVin1-C6a</i>
36	HX293	GanSu	22.82	<i>AnVin1-C6a</i>	92	HX339	ShanXi	31.08	<i>AnVin1-C6a</i>
37	HX308	ShanXi	22.84	<i>AnVin1-C6a</i>	93	HX262	Inner Mongolia	31.06	<i>AnVin1-C6a</i>
38	HX92	ShanXi	22.89	<i>AnVin1-C6a</i>	94	HX127	Canada	31.02	<i>AnVin1-C6a</i>
39	HX358	ShanXi	22.90	<i>AnVin1-C6a</i>	95	HX278	QingHai	30.89	<i>AnVin1-C6b</i>
40	HX144	Japan	22.93	<i>AnVin1-C6b</i>	96	HX295	GanSu	30.81	<i>AnVin1-C6a</i>
41	HX271	Inner Mongolia	22.98	<i>AnVin1-C6a</i>	97	HX334	ShanXi	30.73	<i>AnVin1-C6a</i>
42	HX306	Inner Mongolia	23.01	<i>AnVin1-C6a</i>	98	HX108	YunNan	30.61	<i>AnVin1-C6a</i>
43	HX93	JiLin	23.08	<i>AnVin1-C6a</i>	99	HX266	Inner Mongolia	30.35	<i>AnVin1-C6a</i>
44	HX112	SiChuan	23.18	<i>AnVin1-C6a</i>	100	HX273	Inner Mongolia	30.33	<i>AnVin1-C6a</i>
45	HX258	HeBei	23.19	<i>AnVin1-C6a</i>	101	HX314	ShanXi	30.25	<i>AnVin1-C6a</i>
46	HX49	Inner Mongolia	23.32	<i>AnVin1-C6b</i>	102	HX272	Inner Mongolia	30.16	<i>AnVin1-C6a</i>
47	HX309	ShanXi	23.35	<i>AnVin1-C6b</i>	103	HX282	ShanXi	30.14	<i>AnVin1-C6a</i>
48	HX303	HeBei	23.49	<i>AnVin1-C6a</i>	104	HX356	ShanXi	29.91	<i>AnVin1-C6a</i>
49	HX129	Russia	23.53	<i>AnVin1-C6b</i>	105	HX22	HeBei	29.54	<i>AnVin1-C6a</i>
50	HX360	ShanXi	23.57	<i>AnVin1-C6a</i>	106	HX117	SiChuan	29.52	<i>AnVin1-C6a</i>

Table 4 (continued)

Num.	Code	Source	Hardness value/N	AnVin1-C6 allele type	Num.	Code	Source	Hardness value/N	AnVin1-C6 allele type
51	HX364	ShanXi	23.58	<i>AnVin1-C6b</i>	107	HX264	Inner Mongolia	29.51	<i>AnVin1-C6b</i>
52	HX281	ShanXi	23.62	<i>AnVin1-C6a</i>	108	HX94	XiZang	29.50	<i>AnVin1-C6a</i>
53	HX361	ShanXi	23.65	<i>AnVin1-C6a</i>	109	HX62	ShanXi	29.39	<i>AnVin1-C6a</i>
54	HX107	YunNan	23.65	<i>AnVin1-C6a</i>	110	HX80	QingHai	29.37	<i>AnVin1-C6a</i>
55	HX270	Inner Mongolia	23.71	<i>AnVin1-C6b</i>	111	HX342	ShanXi	29.35	<i>AnVin1-C6b</i>
56	HX102	YunNan	23.92	<i>AnVin1-C6a</i>	112	HX298	Inner Mongolia	29.25	<i>AnVin1-C6a</i>

Table 5 Association analysis between *AnVin-1C6* genotype and hardness values of 112 naked oats

	df	SS	MS	F	P-value
Regression analysis	1	43.23	43.23	1.61	0.21
Residual	110	2958.13	26.89		
Total	111	3001.36	–		

Conclusion

In the present study, we found that the structural differences of *A. nuda* with different grain hardness were primarily reflected in the sub-aleurone layer and the internal endosperm. Multiple copies of *AnVin-1* and *AnVin-3* genes exist in *A. nuda*, and their expression

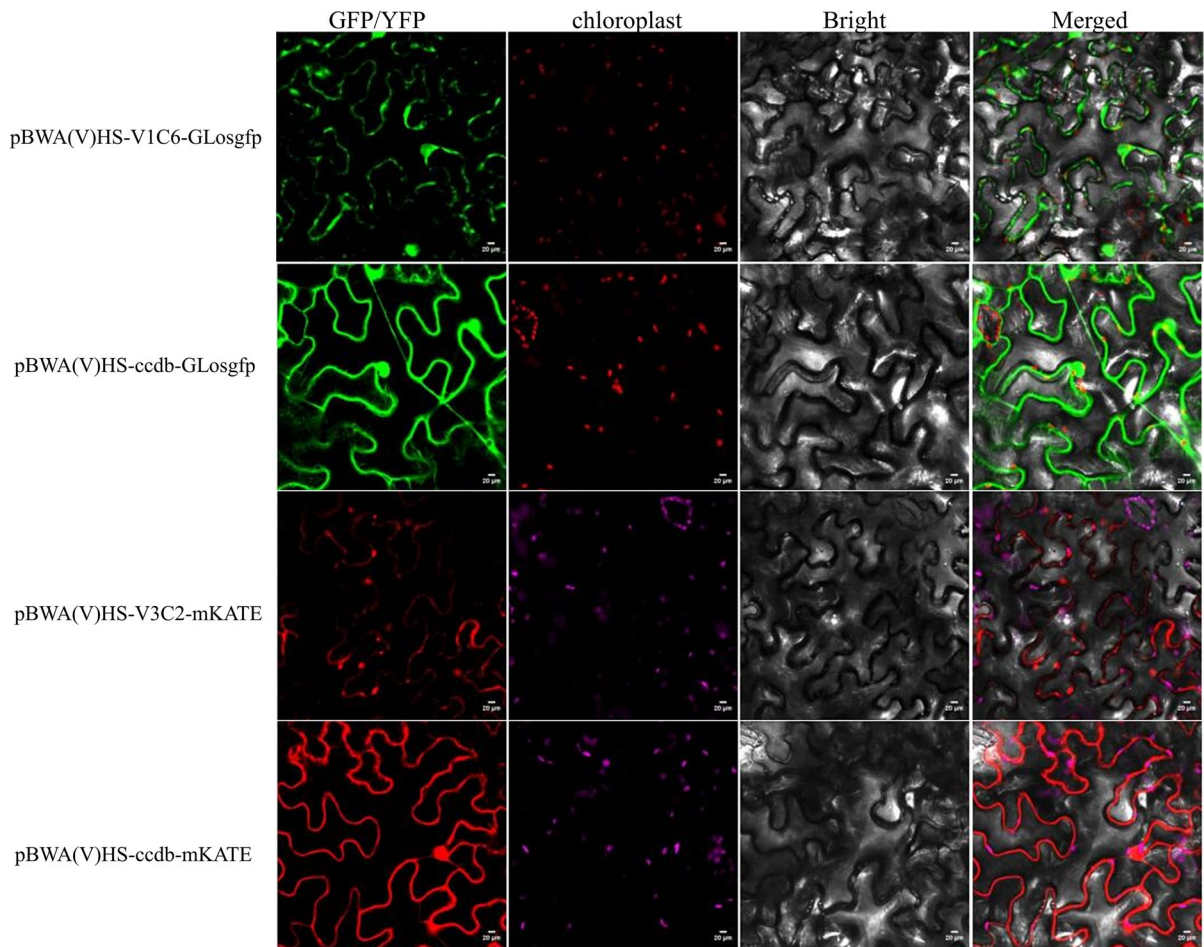


Fig. 14 Subcellular localization of fluorescent-modified *AnVin-1C6* and *AnVin-3C2*

is not seed-specific. The expression levels of the two genes were highest among the 14 DAP seeds. The expression levels of *AnVin-1C* and *AnVin-3C* were higher in soft oat than in hard oat. CAPS marker developed from the two genotypes of the *AnVin-1C6* sequence from the 10 materials could explain 1.44% of the hardness variation.

Discussion

Vin genes are conserved within the genus *Avena*, but research on related genes in *A. nuda* is sparse. In this paper, we focused on the characterization of *Vin*-related genes in *A. nuda*. Both *AnVin-1* and *AnVin-3* had a tryptophan-rich region of “WPWK-WWK,” which is consistent with the structure of indoline proteins. This region is related to its polar lipid affinity to starch (Schibli et al. 2002). Phylogenetic tree analysis found that the *Ain* gene was more closely related to the *Pin* gene in wheat than to the *Vin* gene in oat, consistent with the results of Gazza (Gazza et al. 2015). It was demonstrated that the role of *Ain* gene in oat grain hardness was insignificant through Western blot and that *Vin* had a greater effect on grain hardness than *Ain* (Gazza et al. 2015). The expression differences of *AnVin* in different hardness materials primarily occurred in the C genome, which may be related to its phylogenetic relationships.

The structure of oat kernels consists of seed coat, pericarp, aleurone layer, subaleurone layer and starchy endosperm. From the perspective of cell structure, the cell size of the aleurone layer is similar, which is consistent with Zhang Ruiqi’s research (Ruiqi et al. 2011) on the relationship between the hardness of wheat grains and their microstructure, which found that there is no significant difference in the aleurone layer of wheat grains with different hardness. The morphology and arrangement of the subaleurone layer will have a significant impact on the grain hardness, and the arrangement of the endosperm cell structure will affect the grain firmness. From the perspective of microstructure, the aleurone layer cells of soft oats are arranged neatly, while the cells of hard oats are more disorderly. The endosperm structure of hard oat was tight, and the starch granule was full. The protein and starch granule, starch granule and starch

granule squeezed each other. The void was small, and the starch granule showed irregular shape. The starch granules in soft oats are loosely arranged, and there are large gaps between protein and starch granules, and between starch granules. The tightness of protein and starch granules is related to hardness, which is consistent with the research conclusion of wheat hardness (Ma et al. 2016).

CAPS Marker is a molecular marker technology that combines PCR and enzyme digestion technology, and a relatively simple method to detect SNPs site variation. Restriction endonucleases can recognize the difference of a single base, and the polymorphism of the restriction site can be used to establish the target. In this study, although there are multiple SNP sites, some SNPs do not cause changes in the recognition sites of restriction endonucleases, so that multiple sites cannot be directly detected by endonucleases. The developed CAPS marker only explained 1.44% of the phenotypic variation rate, which may be related to the gene conservation and population size. The verification of molecular markers of grain hardness needs to be further carried out in larger natural populations or recombinant inbred lines.

We found that the *AnVin* gene had high sequence similarity in materials with different hardness values. Polymorphisms caused difficulty in developing specific primers. Due to the high homology of each sequence, ARMS-PCR method was used to design primers (Yijia et al. 2013). The *AnVin-1* was not seed-specific, indicating *AnVin-1* might also function in other tissues. Puroindoline (PIN) was shown to inhibit growth and kill a variety of bacteria and fungi (Morris 2019). PINA can rupture mycelium cell membranes, damage mitochondria, and fragment or translocate DNA of *Aspergillus flavus*, thereby affecting the storage characteristics of wheat (Ang 2020). The antibacterial effect of PINA is greater than that of PINB. PIN exerts its antibacterial effect primarily by lysing the pathogenic bacterial plasma membrane with specific lipid components (Yingjie 2013). VINs may also have functions similar to PINs and located outside the cell membrane. In this study, we found that the *AnVin-1* and *AnVin-3* proteins may be located in cytomembrane. The results indicated that the *AnVin-1* might be a nucleoprotein and *AnVin-3* might be a secreted protein. *AnVin-1* and *AnVin-3*

may work in different ways in the mechanism of grain hardness formation in naked oat.

We present a preliminary investigation of *AnVin* genes in *A. nuda*, using *Vin* genes as comparator references, which will provide information for future research on the grain texture of *A. nuda*.

Acknowledgements Thanks to the Institute of Crop Science, Chinese Academy of Agricultural Sciences for providing a portion of the oat materials.

Author contributions All authors contributed to the study conception and design. Material preparation, data collection, and analysis were performed by JA, JN, MC, HL, YY, and BH. The first draft of the manuscript was written by JA, and all authors commented on previous versions of the manuscript. All authors read and approved the final manuscript.

Funding We appreciate the funding support from National Key Research and Development Project of China (2022YFE0119800), Funding form Key Laboratory of Germplasm Innovation and Utilization of Triticeae Crops at Universities of Inner Mongolia, and team funding of the School of Life Sciences of Inner Mongolia Agricultural University (TD202103).

Declarations

Conflict of interest The authors declare that they have no conflict of interest.

Open Access This article is licensed under a Creative Commons Attribution 4.0 International License, which permits use, sharing, adaptation, distribution and reproduction in any medium or format, as long as you give appropriate credit to the original author(s) and the source, provide a link to the Creative Commons licence, and indicate if changes were made. The images or other third party material in this article are included in the article's Creative Commons licence, unless indicated otherwise in a credit line to the material. If material is not included in the article's Creative Commons licence and your intended use is not permitted by statutory regulation or exceeds the permitted use, you will need to obtain permission directly from the copyright holder. To view a copy of this licence, visit <http://creativecommons.org/licenses/by/4.0/>.

References

Alfieri M, Gazza L, Pogna NE, Redaelli R (2014) Gene sequences of vromindolines in *Avena* species. *Genet Resour Crop Evol* 61(8):1481–1490. <https://doi.org/10.1007/s10722-014-0123-4>

Ang L (2020) Expression of wheat PINA protein in vitro and its antifungal effect against *Aspergillus Flavus*. Dissertation, Henan University of Technology

Chunqing Z (1992) Study on relation between texture and chemical composition of wheat. *Food Storage* 21(1):33–38

Gazza L, Taddei F, Conti S, Gazzelloni G, Muccilli V, Janni M (2015) Biochemical and molecular characterization of *Avena* indolines and their role in kernel texture. *Mol Genet Genom* 290(1):39–54

Giroux MJ, Morris CF (1998) Wheat grain hardness results from highly conserved mutations in the friabilin components puroindoline a and b. *Proc Natl Acad Sci USA* 95(11):6262–6266

Greenwell P, Schofield JD (1986) A Starch granule protein associated with endosperm softness in wheat. *Cereal Chem* 63:379–380

Jianghong A (2022) Grain hardness and allelic variation and hardness related molecular marker development of *Vin-1/3* genes in *Avena nuda*[D]. Inner Mongolia Agricultural University

Jianghong A, Wenjing Z, Yinglin Z, Bing H, Jinsheng N (2020) Research progress on grain hardness of wheat crops. *J North Agric* 48(4):40–47

Jianghong A, Wenjing Z, Xiaohong Y, Jinsheng N, Yan Y, Mingxia Y, Bing H (2021) Comparison of two methods for kernel hardness determination of naked oats. *Crops* (06): 28–35

Ma D, Qin H, Ding H, Jian Z, Guo T (2016) Surface lipids play a role in the interaction of puroindolines with wheat starch and kernel hardness. *Cereal Chem* 93(5):523–528

Morris CF (2019) The antimicrobial properties of the puroindolines, a review. *World J Microbiol Biotechnol Bull* 35(6):86. <https://doi.org/10.1007/s11274-019-2655-4>

Ruiqi Z, Man R, Shouzhong Z, Lin H, Weigang X (2011) Relationship between the wheat grain hardness and the endosperm composition and microstructure in a RIL population. *Sci Agric Sin* 9:1753–1762

Schibli DJ, Epand RF, Vogel HJ, Epand RM (2002) Tryptophan-rich antimicrobial peptides: comparative properties and membrane interactions. *Biochem Cell Biol* 5:80

Shihua G (2003) Biochemical and molecular markers of grain hardness in chinese common wheat (*Triticum aestivum* L.). Dissertation, Shandong Agricultural University

Shihua G, Zhonghu H, Qing M, Honggang W (2005) Wheat grain hardness review. *J Triticeae Crops* 25(2):107–111

Sourdille P, Perretant MR, Charret G, Leroy P, Bernard M (1996) Linkage between RFLP markers and genes affecting kernel hardness in wheat. *Theor Appl Genet* 93(4):580–586

Tao Y, Shanshan S, Shiqing G, Yimiao T, Changping Z (2013) Cloning of *AsRBP1* gene from oat and analysis on its expressions to stresses. *J Triticeae Crops* 33(02):217–223

Turaki AA, Ahmad B, Magaji UF, Abdulrazak UK, Yusuf BA, Hamza AB (2018) optimised cetyltrimethylammonium bromide (ctab) dna extraction method of plant leaf with high polysaccharide and polyphenolic compounds for downstream reliable molecular analyses. *Afr J Biotechnol* 16(24):1354–1365

Yijia Z, Yanying Q, Yuanyuan X, Quanjia C, Wenlin F, Shuniao M, Weiwei L (2013) A Study on cotton SNP typing by ARMS-PCR. *Xinjiang Agric Sci* 50(12):2182–2188

Yingjie M. (2013) Construction, expression and antibacterial activity analyses of wheat puroindoline a artificial mutants and its functional analyses in transgenic wheat. Dissertation, Huazhong University of Science and Technology

Publisher's Note Springer Nature remains neutral with regard to jurisdictional claims in published maps and institutional affiliations.